Published 03/28/2017

doi:10.4271/2017-01-1546
saepcmech.saejournals.org

Aerodynamic Analysis of Grand Prix Cars Operating in Wake Flows

Joshua Newbon and David Sims-Williams
Durham University

Robert Dominy
Northumbria University

ABSTRACT

The effect of the upstream wake of a Formula 1 car on a following vehicle has been investigated using experimental and computational methods. Multiple vehicle studies in conventional length wind tunnels pose challenges in achieving a realistic vehicle separation and the use of a short axial length wake generator provides an advantage here. Aerodynamic downforce and drag were seen to reduce, with greater force reductions experienced at shorter axial spacings. With lateral offsets, downforce recovers at a greater rate than drag, returning to the level for a vehicle in isolation for offsets greater than half a car width.

The effect of the wake was investigated in CFD using multiple vehicle simulations and non-uniform inlet boundary conditions to recreate the wake. Results closely matched those for a full two-vehicle simulation provided the inlet condition included unsteady components of the onset wake. Creating a nonuniform inlet condition allowed the wake parameters to be modified to test sensitivity to different wake features. Dynamic pressure deficit in the wake is shown to have the greatest impact on the following vehicle, reducing loading on the downforce producing surfaces. Wake up-wash and vortex flows are shown to have a smaller effect on downforce generated by the following car, but have an important role in diverting the dynamic pressure deficit upwards and over the following car.

Future regulation changes, aimed at reducing the downforce loss experienced when following another car, should aim to reduce the velocity deficit onset to the following car; either by reducing wheel and underbody wakes, or by extracting the wake using up-wash from the rear wing.

CITATION: Newbon, J., Sims-Williams, D., and Dominy, R., "Aerodynamic Analysis of Grand Prix Cars Operating in Wake Flows," *SAE Int. J. Passeng. Cars - Mech. Syst.* 10(1):2017, doi:10.4271/2017-01-1546.

INTRODUCTION

Grand Prix cars are the fastest circuit racing vehicles. The regulations [1] enable high power and low vehicle weight which leads to the cars being grip-limited. A key performance enabler for these vehicles is aerodynamic performance (especially downforce), enabling peak braking force exceeding 5g, with sustained lateral load of over 4g possible [2]. Aerodynamics is also recognized as a key performance differentiator between cars [2, 3, 4].

As key improvements to lap-time can be made by teams through development of the aerodynamic performance of the cars, the development of Grand Prix cars is shrouded in secrecy with few studies published by Formula 1 teams. Those which are tend towards summary of methodologies, such as CFD capabilities and use of PIV in wind tunnel testing to identify flow features around the car [3, 4, 5, 6, 7], rather than describing the minutiae of designs [8]. As such, most published literature related to Grand Prix car aerodynamics is from academic institutions, and tends toward investigation of subsystems of the cars.

Aerodynamic downforce in Grand Prix racing is generated through inverted front and rear mounted wings, and a sculpted underbody with up-swept rear diffuser [9] (Figure 1), and exceeds vehicle weight above ~150km/h [10], depending on circuit characteristics. Downforce generated by the front wing and underbody are enhanced by ground effect. As well as peak downforce, the location of the downforce center-of-pressure is important as it determines the handling balance. Downforce acting through the rear axle aids traction and stability, while downforce on the front axle aids steering. The relative location of the center of gravity and center of pressure determines how the vehicle steer characteristic will change with speed. Too little front downforce causes the car to understeer at higher speeds, while too little rear downforce results in oversteer at higher speeds. Aerodynamic balance may be described by the percentage of total downforce acting on the front axle,

$$Aero.balance = \frac{C_{Lf}}{C_L} \times 100 \quad (1)$$

and values between 35% and 45% [3, 11] are generally considered optimal, depending on circuit characteristics and the location of the car's center-of-gravity. Current F1 regulations dictate a centre of gravity balance of 46% on the front wheels for a car of minimum weight [1] and it is normal to place the center of pressure slightly behind the center of gravity.

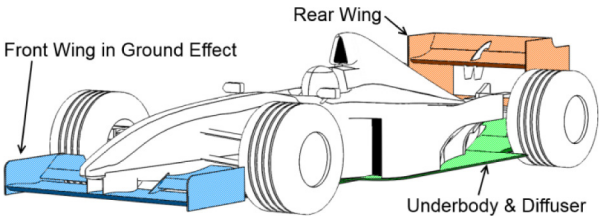

Figure 1. Grand Prix car with downforce generating features labelled

The wake of a Grand Prix car is dominated by a large counter-rotating vortex pair shed from the rear wing tips [12, 13]. The relatively short span of the wing leads to a strong interaction between the vortices, enhancing the centerline up-wash, while the low height of the wing also constrains flow near the ground, creating a strong horizontal component towards the centerline. The vorticity is coupled with high turbulence intensity, in excess of TI = 45% [12], and low axial velocity. The velocity deficit is swept to the centerline and upwards to surround the vortex cores, creating a "mushroom" shaped wake.

The effect of an upstream vehicle on a downstream Grand Prix car is a reduction of aerodynamic downforce, up to 36%, and aerodynamic drag, up to 23% based on an early 1990s car [14] (17% and 10% respectively in the mid to late 2000s [15]). Reductions of drag increase straight line speed, and are beneficial in effecting an overtake, known as slipstreaming or drafting. However, reductions of downforce are concentrated on the front axle, reducing the front aero-balance by up to 22%. The shift of balance results in understeer, which compounds the lower cornering velocity from reduced downforce with increased tire wear. Recovery of downforce and drag toward their baseline values occurs with a lateral offset between vehicles [14]. Recovery of downforce occurs more rapidly than drag, with drag loss exceeding downforce loss for offsets greater than ~0.25 car widths.

The drawback to two vehicle slipstreaming studies in conventional length wind tunnels is the effect of model length on the achievable separation [14, 16, 17]. In order to achieve more representative vehicle separations, requires reduced model scale, which reduces Reynolds number accuracy.

The use of short axial length bluff bodied wake generators have been pioneered in recent years to increase vehicle axial separation, without compromising model scale. The wake generators feature a short bluff body with rear upswept diffuser, a rear wing and wheels [12, 18, 19, 20, 21, 22, 23, 24, 25]. The key features in the wake are recreated to an acceptable level of accuracy, namely the counter-rotating vortex pair and velocity deficit. The effect of the bluff body wake on a downstream car is similar to that of an upstream vehicle at similar vehicle separations [18, 19].

The effect of wakes from bluff bodies on isolated wings in ground effect has also been investigated [12, 20, 21, 22, 23, 24]. Downforce generated by the wings decreased for all ride heights and incidences, though the stall incidence increased [12]. It was found that reducing the angle of the upstream diffuser created a smaller magnitude up-wash which led to higher lift-to-drag ratios of the downstream wing, though these were still significantly lower than the potential freestream efficiency [23].

Changes to the regulations are normally used to reduce downforce, thereby limiting vehicle speeds to improve safety. In 2009 the regulations were changed with the specific intention to improve the performance when following another car [4, 6]. Key targets were to reduce downforce by as much as 50%, while reducing turbulence from the wake. While the changes did result in a "cleaner" wake [15], they did not necessarily have the desired effect on overtaking, even increasing the downforce loss experienced by the following vehicle [15]. Such is the rate of progress in Formula 1 that much of the downforce lost at the beginning of 2009 was recovered by the end of that season [4] and the rear wing drag reduction system (DRS) was introduced ahead of the 2011 season [2, 13, 26] in a further attempt to improve overtaking.

METHODOLOGY

Experiments utilized both wind tunnel and CFD methodologies, with each providing complementary capabilities - rather than competing with each other to provide the same data. Wind tunnel tests allowed time-efficient ride height mappings and (in this case) variation of vehicle separations. CFD allowed direct manipulation of the wake impacting on the vehicle, minimal "tunnel interference" effects and more detailed flow investigation information. Experiments were performed in the Durham University 2m wind tunnel, which features a 3.1m × 1.4m rolling road for automotive applications. Tests utilized a 25% scale Grand Prix car model (Figure 1) at a Reynolds number of 2.05×10^6. based on model length. To simulate an upstream vehicle a short axial length wake generator, Figure 2, was placed on the rolling road at a number of locations ahead of the test car.

Vehicle body forces were measured using an internal 6-component balance, connected via a numerically controlled overhead strut which controls ride height and model pitch. Wheels were mounted externally with individual drag load cells for each corner. Load cells were connected to a bank of Fylde FE-579 strain gauge amplifiers, with total repeatability of ±0.002 on C_D and ±0.006 on C_L. The model also featured 120 surface pressure tappings in the front wing and underbody, which were measured using a Scannivalve ZOC33/64PxX2 electronically scanned pressure transducer bank.

The coordinate system used corresponds to SAE J1594 [27] with x=0 corresponding to the front of the vehicle for cases with a single vehicle. For cases with two vehicles, results are presented in terms of vehicle separation, the distance from the rear of the upstream vehicle to the front of the following vehicle.

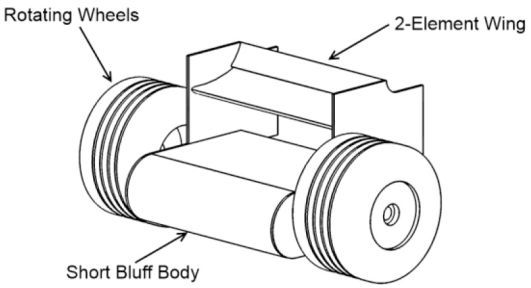

Figure 2. Short axial length bluff bodied wake generator

CFD was performed using PowerFLOW, a Lattice-Boltzmann Method (LBM) solver. Turbulence modelling is performed at grid scale with a LBM-compatible Very Large Eddy Simulation with sub-grid scale turbulence resolved using a two equation, k-ε model. Near wall behavior is approximated by a wall model which accounts for pressure gradient effects, capturing separation behavior. The fluid lattice comprises of voxels, in the fluid volume, and surfels at the surface boundary of a fully detailed geometry. Lattice refinement is controlled by variable resolution (VR) regions with voxel lattice length doubling between VR levels.

Simulations were performed using the same 25% Grand Prix car and Reynolds number as the wind tunnel study, with the inclusion of suspension arms. Cases were run for a single vehicle attitude, corresponding to the peak downforce found in experiments with wheels mounted to the body, a nominal ride height of 4mm, with a nose-down pitch of 0.6°. The mesh contained 1.6×10^7 cells, with minimum cell size of 1.5mm. Simulations required up to 1500CPU hours to compute 0.7s with forces averaged over the final 0.35s, running on the Durham University high performance computer cluster of ~2000 Intel Xeon E5-2650 2.6GHz processors.

ISOLATED VEHICLE (BASELINE)

To determine the effect of an upstream vehicle wake, the aerodynamic forces for the isolated vehicle were measured. A number of ride heights (h_{min}) and nose down pitch/rake angles (θ) were tested, Figure 3, to test sensitivity to changes, and identify the optimum condition. Downforce coefficient ($-C_L$) generated by the car increases with reducing ride height, from ~1.1 to -1.2. It can be seen that car pitch angle does not significantly affect the gradient of force enhancement, but the aero-balance is altered by rake.

While all car conditions fall within the optimal range of 40% to 45% of downforce on the front axle, the aero-balance is affected by car pitch. Flatter vehicle attitudes result in a relatively consistent aero-balance, which gives the driver confidence as the handling does not change as the car brakes, accelerates, and turns. As pitch is increased the aero-balance shifts forwards with reducing ground clearance, this is mainly due to the front wing, which moves closer to the ground plane as pitch increases; while the rear diffuser throat also moves further from the ground, hence why downforce increases linearly regardless of rake angle.

Not shown in Figure 3 is the aerodynamic drag, which is relatively unaffected by attitude ranging from 0.76 to 0.77 on C_D. Approximately half of the vehicle drag is generated by the wheel, with the front and rear wheels each generating ~0.19 on C_D. The optimal condition was identified as the lowest nominal ride height tested (2mm) with no rake (θ=0°) on the car, $-C_L = 1.21$, with an aero-balance of 41.5%. As the optimal setup would be selected for a Grand Prix event, wind tunnel experiments for the car-in-wake were performed using this vehicle attitude.

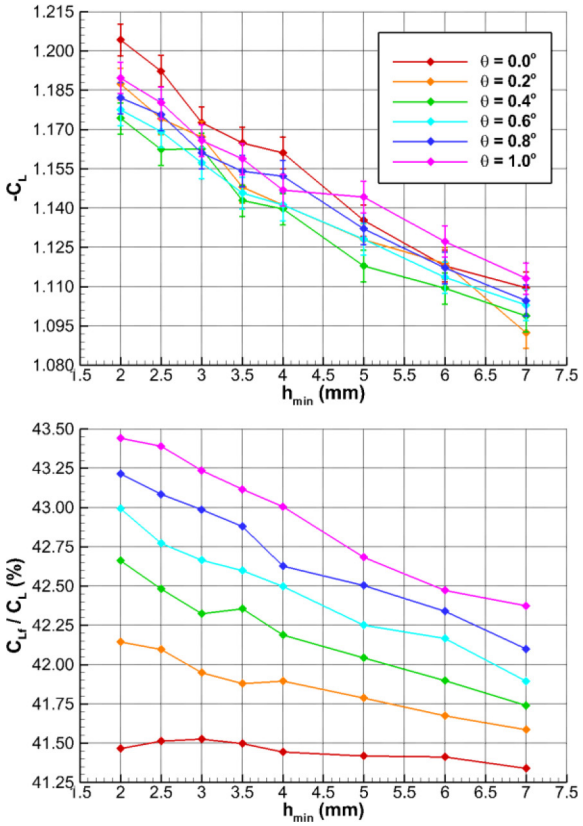

Figure 3. Isolated vehicle downforce and aero-balance (wind tunnel)

Vehicle forces measured with CFD are different to those from experiments (baseline $C_D = 0.92$ and $-C_L = 0.85$, with a more forward aero-balance of 47.5%). The CFD simulations were used to complement the wind tunnels tests, rather than replicate them, and so there are several differences including lift-producing suspension members in the simulation, different blockage conditions, no wind tunnel mounting apparatus etc. The processes of generating downforce can be seen in Figure 4; starting at the front wing, there is a large region of sub-atmospheric pressure on the lower surface ($C_P < 1$). At the front of the floor there is a further peak of low pressure ($C_P \sim -1.5$), with a second peak at the diffuser throat ($C_P \sim -0.6$). The pressure at the diffuser is less negative than the front of the floor, partly due to the generic design producing low downforce, but also as the nose-down pitch moves the rear of the car away from the ground, increasing the area of the diffuser 'throat' (between the ground and the car's floor), limiting the peak dynamic pressure in this region.

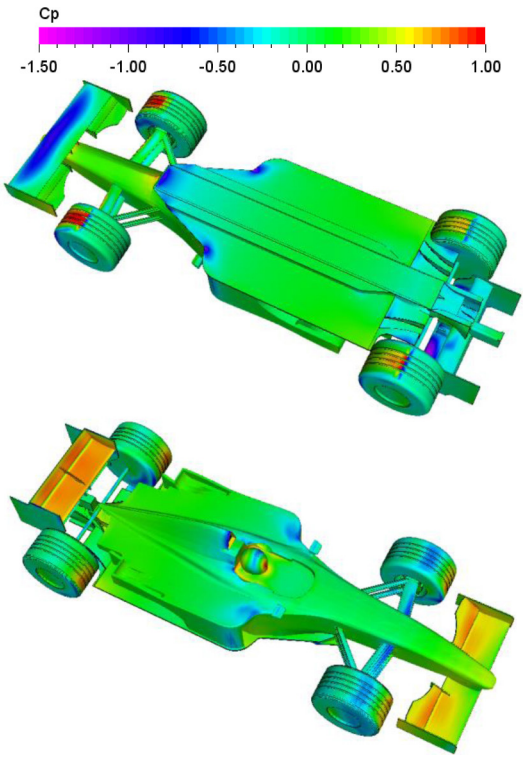

Figure 4. Isolated vehicle surface pressure distribution (CFD)

AERODYNAMIC EFFECT OF AN UPSTREAM VEHICLE

The longest separation achievable in the wind tunnel with both "vehicles" on the moving ground was one vehicle length, which is representative of the spacing between cars prior to an overtaking maneuver; CFD was performed at the same separation with the wake generator and a second full vehicle (Table 1). Aerodynamic drag and downforce of the following vehicle reduce compared to the isolated car, and the aerobalance on the front wheels decreases by up to 11%. The effect on drag is similar between the experimental and CFD, as well as between wake generator and full vehicle. The difference between the effect the wake generator and full vehicle on downforce is slightly greater, albeit only 0.1 on $-C_L$. This gives some confidence in the accuracy of the wake generator, which while not perfect has a similar effect on the aerodynamic performance of a following car.

Table 1. Difference between measured effects of upstream vehicle, with a one vehicle length separation

	ΔC_D	$\Delta(-C_L)$	$\Delta(-C_{Lf})$	Δ Aero. balance
Wake generator (wind tunnel)	-0.15	-0.45	-0.19	-1%
Wake generator (CFD)	-0.16	-0.41	-0.24	-11%
Full upstream vehicle (CFD)	-0.18	-0.51	-0.26	-5%

Component forces from CFD are shown in Figure 5, the figure highlights the negative impact of the exposed wheels, accounting for 35% of the vehicle drag while also generating a positive lift. The effect of the wake on wheel drag and lift as a percentage of the baseline is small compared to the rest of the car. Contrary to conventional thinking, of the downforce generating bodies, the front wing is least affected by the upstream wake, especially the front wing drag, which in barely affected by the presence of the upstream car, $\Delta C_D = -0.006$. The rear wing is the most affected by the upstream wake, losing -0.182 on $-C_L$, downforce and drag lost by the rear wing is also approximately proportional, losing ~55% compared to the baseline.

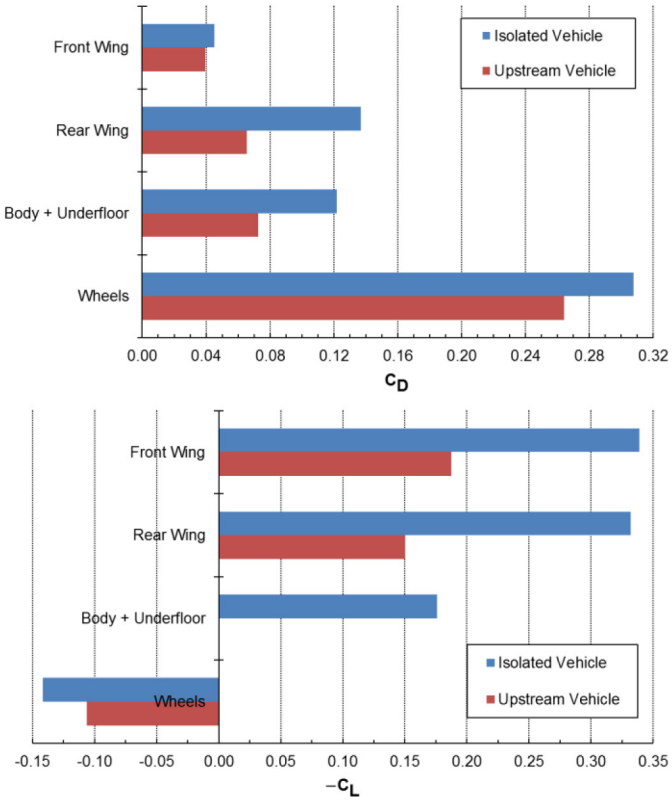

Figure 5. Breakdown of non-dimensional component force coefficients, based on frontal area (CFD)

The effect of the full upstream vehicle, with a one vehicle separation, on the surface pressure distribution is shown in Figure 6. Regions of low pressure, such as the lower surfaces of the front and rear wings, and front of the underbody and rear diffuser, all experience an increase of pressure, $\Delta C_P > 1.0$; while high pressure regions, like the upper surfaces of the wings, experience a reduction of static pressure, $\Delta C_P < -0.8$. The regions of peak, high and low, pressure experience the greatest change, with little effect on the regions where $C_P \sim 0$ effectively squeezing the peak pressures ($\pm C_P$) towards zero.

While peak changes in pressure on the front wing and underbody are of similar magnitude, the planform area of the underbody significantly exceeds the front wing, $A_{underbody} \sim 5.7 \times A_{front\ wing}$ and hence the downforce loss on the underbody is the more significant. The majority of the effect of the upstream wake on the underbody is towards the leading edge, which contributes to the reduced front aero-balance despite the fact that the rear wing actually loses slightly more downforce than the front wing.

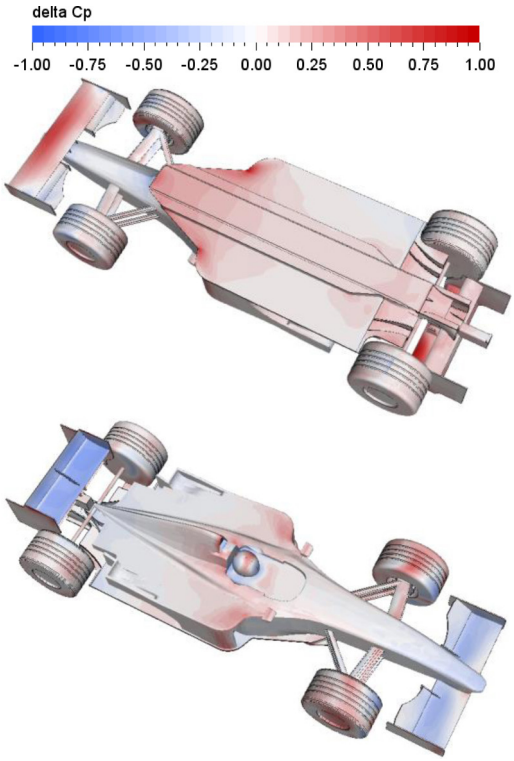

Figure 6. Effect of upstream vehicle on surface pressure coefficient on following vehicle (CFD)

An advantage of wind tunnel testing with a wake generator, compared with CFD, is the capability to efficiently test a number of inter-vehicle separations, with a number of vehicle conditions. Longitudinal separations between 0.2 and 1.0 car lengths were tested with corresponding lateral offsets up to 0.75 car widths (W), Figure 7. The greatest loss of downforce and drag both occur when the two vehicles are aligned along their centerlines, with the reduction of force increasing as the axial separation is reduced, up to -0.22 on C_D and -0.8 on $-C_L$. At the closest separation, the aero-balance is reduced to just 20%, which would have a significant effect on the handling balance of the car towards understeer.

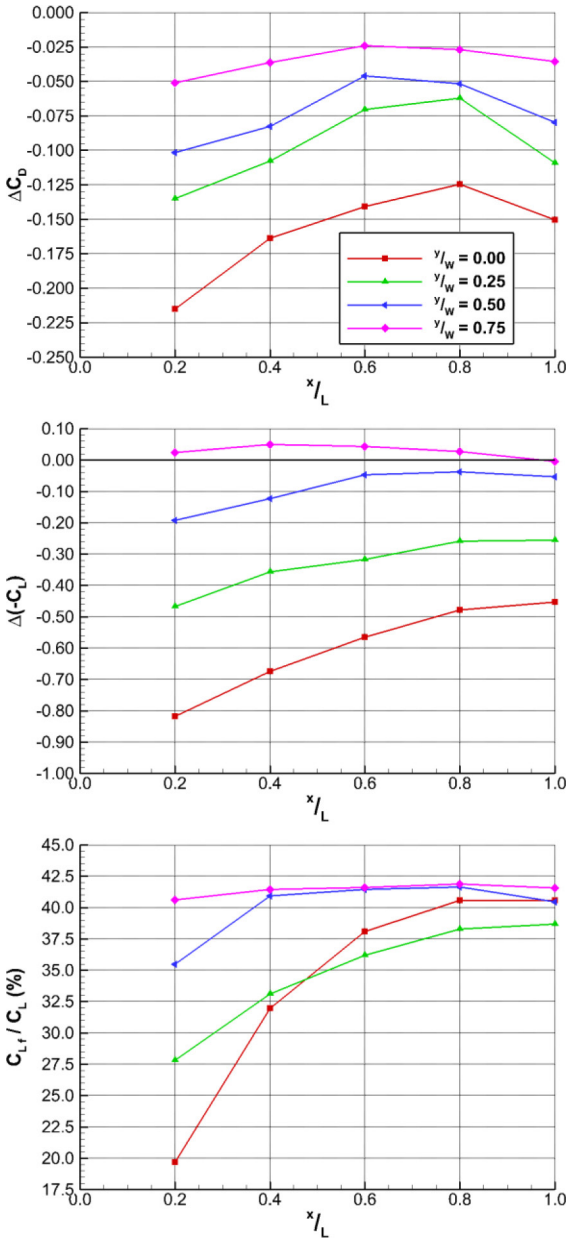

Figure 7. Effect of upstream vehicle on force coefficients of a following vehicle at multiple vehicle separations (wind tunnel)

The effect of reducing the separation on the front wing pressure distribution is shown in Figure 8. As discussed, the effect of the wake with a one car separation is to reduce regions of high suction, the effect of which is greater at the shortest separation, where the quarter-span downforce is reduced to almost nil.

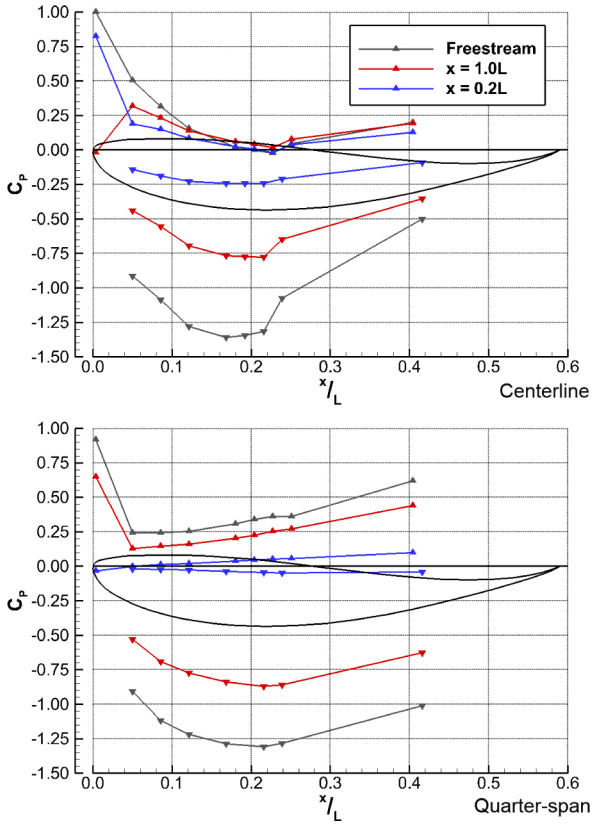

Figure 8. Effect of longest and shortest axially aligned cases on front wing pressure distribution (wind tunnel)

Drag and downforce recover towards their baseline values with just a small, y = 0.25W, lateral offset between the vehicles; the downforce deficit is almost halved for all longitudinal positions tested, while drag increases by ~0.1 on C_D. Increasing the size of the offset reduces the force loss further, as well as reducing the gradient of force loss with reducing axial spacing. Drag remains in deficit for all conditions tested, which would have the benefit of improving top speed compared to the baseline, while downforce actually exceeds the baseline performance for the y = 0.75W offset, probably as a result of the high magnitude wake downwash outboard of the upstream vehicle.

GRAND PRIX CAR WAKE

The wake of the Grand Prix car is dominated by a large region of stagnation pressure deficit coupled with the counter-rotating vortex pair from the rear wing. Static pressure deficit in the wake is low so most of the stagnation pressure deficit is dynamic pressure, resulting from the velocity deficit, Figure 9 & Figure 15, which is present many car lengths aft of the vehicle. At the base of the car the wake velocity deficit is concentrated behind the wheels and rear wing ($u_x \ll 0.2U_\infty$). There is some flow reversal behind the rear wheels, which closes by x = 1.1L (0.1 car lengths behind the rear of the car).

The rear wing vortex pair commences roll up from the leading edge of the endplates as the high pressure above the pressure surface of the rear wing migrates to the relatively lower pressure on the outer face of the endplate.

The dominant vortex pair produces a strong centerline upwash, with strong in-wash near the ground. The velocity deficit from behind the rear wheels is swept towards the centerline by the in-wash, and upwards to circulate the vortex cores by the up-wash, creating a "mushroom" shaped wake. By x = 2L the in-wash near the ground reduces the width of the wake below the axle height, while diffusion of the vortex cores increases the size of the "mushroom cap". The lowest magnitude velocity deficit surrounds the vortex pair ($u_x < 0.5U_\infty$) at rear wing height.

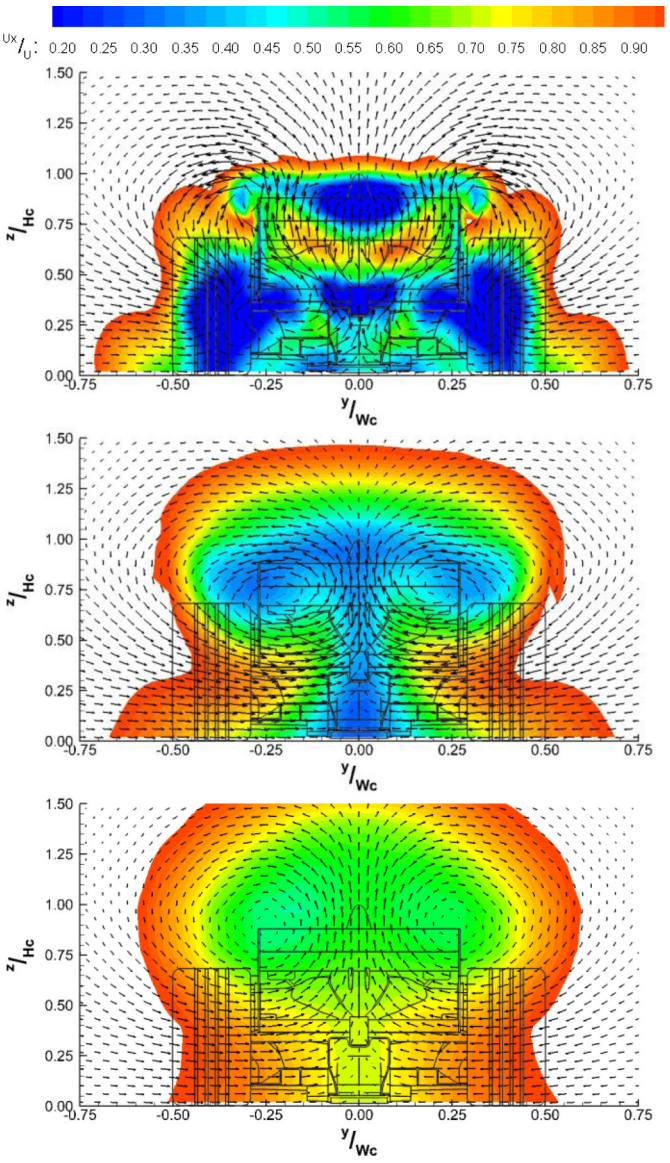

Figure 9. Contours of axial velocity in wake of Grand Prix car, 2-d slices at x = L (upper), x = 1.5 (middle), & x = 2.0L (lower) (CFD)

EFFECTS OF SALIENT WAKE FEATURES

The net effect of an upstream car has been measured and it is possible to identify reasons for impacts (eg: upwash and velocity deficit in the wake of the upstream vehicle). However, there has been limited work to actually evaluate the relative importance of these different wake elements. This is important because different wake characteristics are closely linked to the specification of the upstream vehicle (drag, downforce and proportion of downforce generated out of ground effect). Therefore, the effects of the wake features are analyzed here using a first principles approach.

Effects on Front Wing Downforce

The downforce generated by a 2D airfoil can be calculated from a pressure distribution by the integral of the difference in pressure between upper and lower surfaces over the chord,

$$-C_L = \frac{1}{c}\int_0^{x=c} (C_{P\ Lower} - C_{P\ Upper})\, dx \tag{2}$$

Downforce generate on the front wing mainplane can therefore be calculated, $-C_L = 0.96$ on the centerline, and $-C_L = 0.82$ at the quarter-span.

Up-wash in the wake will result in a reduction of the effective incidence (α) of the front wing. The effect of which can be approximated from the lift slope (a),

$$\Delta C_L = a\, \Delta\alpha, \tag{3}$$

assuming the infinite lift slope (a_∞) is equal to 2π, the gradient of the slope with finite span is approximated using the standard analytic solution from lifting line theory:

$$a = \frac{a_\infty}{1 + {a_\infty}/{\pi\lambda}} \tag{4}$$

where λ is the aspect ratio. The change in effective incidence is equal to:

$$\Delta\alpha = ATAN\left(\frac{u_z}{U_\infty}\right). \tag{5}$$

The up-wash is strongest on the wake centerline (Figure 9), and reduces the effective incidence of the front wing by up to 6° at x = 0.4L, or a predicted change in downforce of up to -0.5 on $-C_L$. Even at this location with the most extreme upwash the expected impact is significantly below the measured change of -0.9 on $-C_L$ for the front wing at this inter-vehicle separation.

The effect of velocity deficit is a reduction in force proportional to the reduction in dynamic pressure. By measuring the axial and vertical velocities in the wake at front wing height and the same separations downstream of the rear of the car as the slipstreaming study, the effect of up-wash and axial velocity deficit could be determined, Figure 10 and compared to the measured effect of the upstream vehicle. Like the full vehicle, Figure 6, the front wing downforce reduces with proximity to the lead car, up to -0.9 on $-C_L$. Both the analysis of effective incidence and velocity deficit match the trend of the whole wake, as would be expected both up-wash and velocity deficit are strongest close to the rear of the lead car (Figure 15).

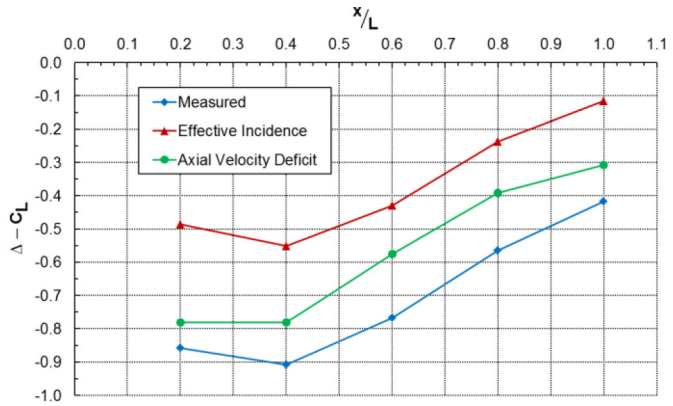

Figure 10. Comparison of theoretical effects of relative incidence and velocity deficit on front wing centerline integral force coefficient (wind tunnel)

The effect of velocity deficit is much closer to the measured effect for all separations. This shows that while up-wash does have an effect on the following vehicle, this effect is much smaller than that of velocity deficit, and is also localized to the centerline of the upstream vehicle.

Effects on Pressure Distribution

The effect of the wake has been shown to be a reduction of peak suction on the front wing as well as over the surface of the car. The effect on surface pressure will be a function of the various wake features, static and dynamic pressure deficits and incidence,

$$\Delta C_P = f(\Delta P, \Delta q, \Delta\alpha) \tag{8}$$

Figure 11 illustrates the observed pressure distributions on the front wing in the baseline (single vehicle) case and behind an upstream vehicle. These are compared with the pressure distribution that would be achieved due to a reduction in dynamic pressure. A significant change in onset static pressure would result in a vertical translation of baseline pressure distribution, which is not seen in the pressure plots. A strong impact from a change in incidence would bring the pressure and suction surface pressures closer together, but the highest pressure on the airfoil would still be at the stagnation pressure. Again this does not fit the observation, where the pressure at stagnation is reduced in line with the scaling of pressures elsewhere. Hence the nature of the change in the pressure distribution is consistent with the impact of reduced dynamic pressure (and onset stagnation pressure) with little change in onset static pressure.

The blue curves in Figure 11 show an expected pressure distribution obtained by scaling the pressure distribution according to the dynamic pressure deficit in the wake (Figure 9) at points measured at the height of the front wing and this shows reasonable agreement with the actual pressure distribution. The stagnation point pressure reduces to C_p ~0.5 and the upper and lower surface pressures are squeezed toward neutral pressure. Pressure on the lower surface is less well recreated by a uniform scaling, even so the integral of the distribution accounts for 90% of the measured reduction of downforce.

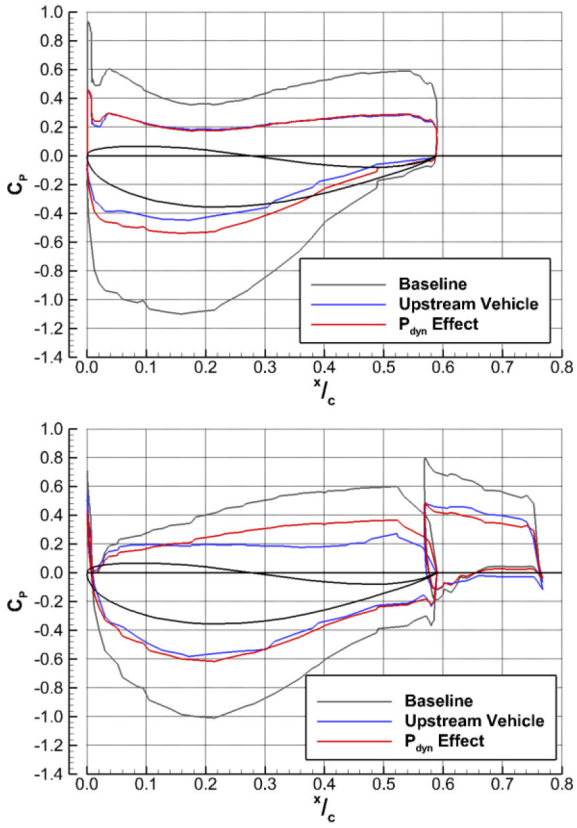

Figure 11. Effect of dynamic pressure deficit scaling, representative of a one vehicle length separation, on front wing centerline and quarter-span pressure distributions (CFD)

Downforce reduction on the front wing becomes less severe further from the wake centerline; likewise dynamic pressure deficit is most significant on the wake centerline. As for the centerline, the correlation between scaling the wake deficit and the measured effect of the wake is similarly close when considering the quarter-span position. Unlike the centerline, the lower surface better matches the measured than the upper; which features a flattening of the pressure distribution along the upper surface. While not the only mechanism at work, the predominant effect can be attributed to that of the dynamic pressure deficit.

Applying the same dynamic pressure scaling to the whole vehicle surface, Figure 12, like the front wing, shows similarities to the effect of a full upstream vehicle (Figure 6). While the peak change of pressure may not exactly match the real wake, the regions where change occurs are the same, namely the upper and lower surfaces of the wings and regions of high peak pressure on the upper and underbody. Using the dynamic pressure across the car at front wing height means the effect on the rear wing is smaller than the real wake, where dynamic pressure deficit is concentrated around the trailing vortices (Figure 9).

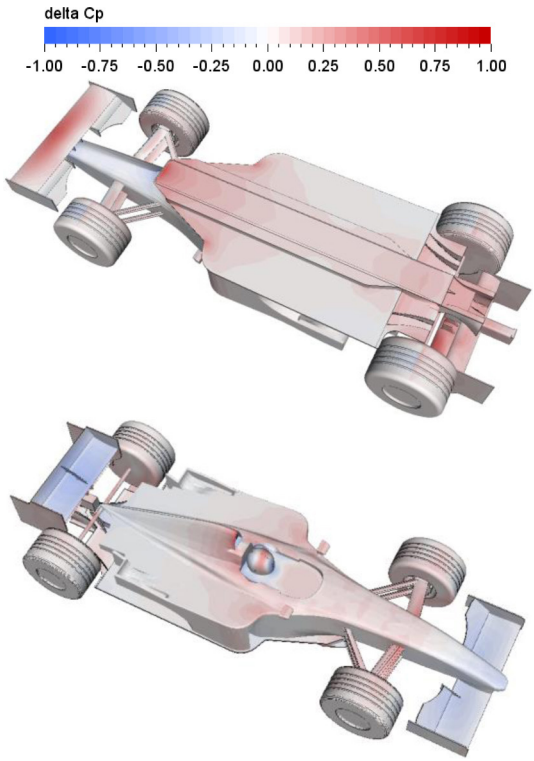

Figure 12. Effect of dynamic pressure deficit scaling, representative of a one vehicle length separation, on vehicle surface pressure distribution (CFD)

A pure dynamic pressure effect would result in equal scaling of both drag and downforce, downforce loss exceeds drag (as a percentage of the baseline) significantly (Table 2) for the whole car. The only component for which drag and downforce scale uniformly is the rear wing, which could be as it operates in a more uniform region of axial velocity deficit in the wake, Figure 9. While it cannot be said that dynamic pressure is the only source of loss for the following car, it appears to be the largest contributor to downforce loss.

EFFECT OF ALTERING WAKE CHARACTERISTICS ON DOWNSTREAM VEHICLE

One advantage of CFD over wind tunnel experiments is the ability to impose a set of non-uniform boundary conditions on the inlet to simulate the upstream wake. This allows the wake to be simply and systematically modified, to test sensitivity to the salient wake features, without the necessity to develop a new vehicle to produce the desired wake.

To simulate an upstream car the wake was sampled behind the isolated vehicle, at such a distance that reversed flows had closed, Figure 16; with the wake sampled at x=1.25L and the inlet set x= -0.75L ahead of the car it was possible to simulate a one car length separation, to match the largest separation tested in the wind tunnel. The sampled wake was imposed on the inlet plane of a second CFD

case, using a static pressure and velocity boundary condition to recreate the wakes axial velocity and static pressure deficits. This methodology is described in more detail in [28]. The sum of static and dynamic pressure deficits generated the stagnation pressure deficit, while the vorticity was recreated using vectors of u_y and u_z.

Table 2 compares the results from simulations with a sampled wake imposed on the inlet with a full two vehicle simulation. The inlet wake was imposed both as a steady wake corresponding to the time-average of the upstream vehicle wake and as a time-varying inlet boundary conditioning based on sampling the upstream wake with a resolution of 1 kHz. The case with the time-resolved inlet wake shows excellent agreement (within 1%) with the full two-vehicle simulation. With a time-averaged inlet wake the drag is in good agreement but the lift is not.

Because the inlet wake is imposed in terms of velocities it is reasonable to expect a difference due to the fact that time-averaging the inlet velocity does not necessarily reproduce the time-averaged dynamic pressure:

$$0.5\rho\overline{u_x}^2 \neq \frac{1}{n}\sum_{t=0}^{n} 0.5\rho\left(u_x(t)\right)^2. \tag{10}$$

However, the fact that the effect on drag is reproduced by the time-averaged inlet wake but the effect on lift is not reveals that there is an important coupling between multiple unsteady parameters, for example, between the path and intensity of the wake.

Table 2. Effect on vehicle forces from altering imposed boundary conditions on following vehicle, compared to isolated vehicle (CFD)

	ΔC_D	ΔC_D (%)	$\Delta - C_L$	$\Delta - C_L$ (%)
Full upstream vehicle	-0.18	-19.3	-0.51	-59.4
Imposed wake – steady inlet	-0.17	-18.3	-0.54	-66.7
Imposed wake – time varying inlet	-0.17	-18.6	-0.52	-58.9
Imposed Wake – no u_x deficit	-0.08	-9.89	-0.24	-37.0
Imposed Wake – no u_y or u_z	-0.33	-41.4	-0.45	-69.3

The simplest modification to the wake to perform is to remove features from the wake. Removing the axial velocity deficit shows the effect of the rear wing vortex pair in isolation, and would represent a removal of the momentum deficit, or upstream vehicle drag. Drag and downforce effects are reduced by approximately half, which is less than would have been anticipated considering the effect dynamic pressure appears to have on the front wing. The front wing of the car actually experiences a 5% increase of downforce, possibly as a result of downwash in the wake towards the wing tips increasing the effective incidence.

Removing u_y and u_z from the wake results in a doubling of the impact of the upstream vehicle on the drag of the following vehicle, while the downforce loss increases by 10%. The effect on the wake (Figure 17) highlights a benefit of u_y and u_z in the wake, in particular the wake up-wash. Without the up-wash the velocity deficit in the wake hangs at the height of the car, saturating the whole vehicle. The loss of cross-flow also results in a wider wake, whereas when the real wake develops the velocity deficit is swept to the centerline, minimizing the effect.

Where it is instructive to note the impact of completely removing wake elements this is not realistic in practice. Therefore, the sensitivity of a following vehicle to changes in the u_y and u_z was investigated at levels that could be achieved by modifying regulations (eg: on rear wing dimensions and/or vehicle ride height). The magnitude of u_y and u_z on the inlet were scaled by ±5% and ±10%, Figure 13.

With the exception of drag generated by the front wing, which is constant for all secondary flow intensities tested, it can be seen that there is a linear relationship between the secondary flow intensity and downforce generated by the car. Reducing secondary flows increases the effect of the wake on downforce and drag produced by the downstream car, and conversely increasing the secondary flows reduces the downforce loss.

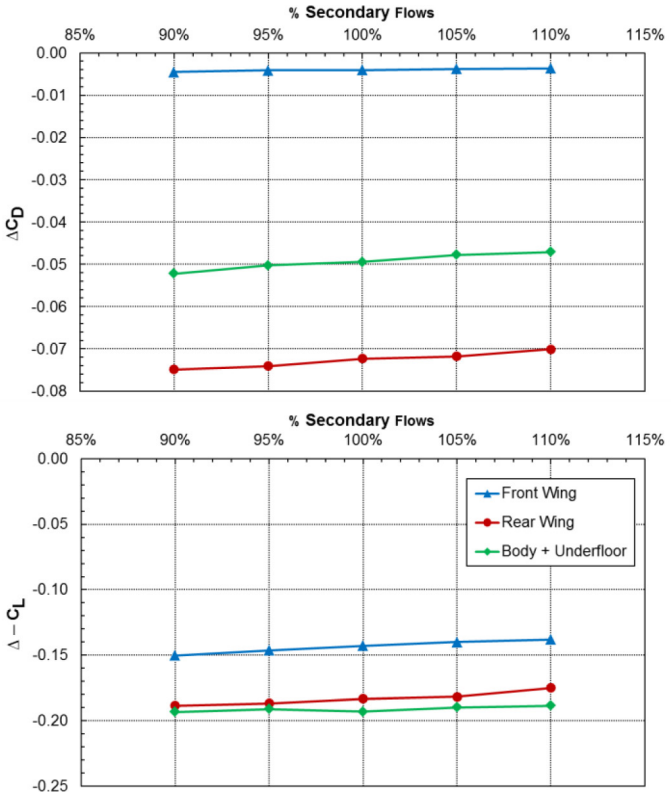

Figure 13. Effect of changing secondary flow intensity on downstream vehicle downforce generation

FRAMING OF FUTURE REGULATIONS TO AID OVERTAKING

The wake of a Grand Prix car is dominated by a large region of stagnation pressure deficit coupled with secondary flows from the rear wing vortex pair, both of which are shown to negatively impact the following car. The most significant of these is the dynamic pressure component of the stagnation pressure deficit, which accounts for as much as 90% of the downforce loss experienced by the front wing.

The body of a Grand Prix car is itself is relatively streamlined, Figure 14, with a narrow rear end which fills in the wake of the wide side-pods, necessary to house cooling radiators and side-on impact protection, with no flow reversal detectable in the wake. Most of the velocity deficit in the wake is the result of the exposed rear wheels and underbody, Figure 9.

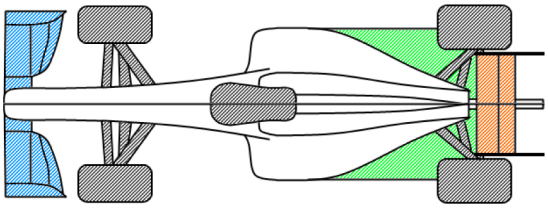

Figure 14. Plan view of Grand Prix car, showing boat-tailing of rear bodywork

Downforce generated by the rear wing in particular generates up-wash in the wake which helps to divert the low velocity wake over the following car. Conversely, downforce generated by the underbody in ground effect implies a low pressure on the ground plane which tends to reduce up-wash, resulting in a wake which remains localized at the height of the following car (see [28]). Modern Grand Prix cars generate as much as 50% of their downforce through the underbody, which could contribute to limited ability of vehicles to follow closely and hence to overtake.

Therefore, a regulation change to reduce the proportion of downforce which is generated in ground effect, with a corresponding increase in downforce from wings out of ground effect could be expected to generate a wake which would have less detrimental impact on the following vehicle. This in turn could be expected to make it easier to follow closely and to increase opportunities for overtaking.

SUMMARY

Aerodynamic downforce and drag are both reduced in the presence of an upstream vehicle; downforce reduces by 38% and drag by up to 20% at representative separations. Force reductions are greatest for the shortest longitudinal separations, with both drag and downforce increasing as the separation is increased. Compounding the loss of downforce is a reduction of percentage of downforce which acts upon the front axle of the following car, causing understeer and increasing the difficulty associated with following and ultimately overtaking a competitor.

Downforce recovers towards the baseline with small a lateral offset to the lead car. Drag remains lower than the baseline, and would aid straight line speed for all lateral offsets tested. The aero-balance is also less severely affected as the lateral spacing increases.

Regions of high, positive and negative, peak surface pressure experience the greatest change with an upstream vehicle, effectively squeezing the surface pressure towards $C_P = 0$.

Analysis, using the dynamic pressure deficit from the wake to scale the pressure distributions of both the front wing and body, showed that a large part of the change in surface pressure can accounted for by the dynamic pressure deficit, as much as 90% on the front wing centerline. Other sources of loss, such as an effective change of incidence from wake upwash, are present, but are less significant than dynamic pressure.

Inlet conditions in CFD were used to recreate the wake of the Grand Prix car. Accuracy was improved by using a time-resolved inlet wake - rather than a time-averaged one. This indicates an important time-varying coupling between wake parameters (eg: variation of wake shape and intensity of dynamic pressure deficit).

Imposing the inlet boundary conditions allowed variables in the wake to be modified, without requiring a change of the vehicle. Removing the vorticity from the wake resulted in a tube of low velocity flow onset to the car, and increased the drag and downforce reductions by 20% and 10% respectively. Conversely removing the axial velocity deficit halved the impact on downforce and drag, compared to an upstream vehicle.

It is clear that while not the only cause of downforce loss on the following vehicle, the dynamic pressure deficit is the most detrimental feature in the wake. Future regulations aimed at improving the capability of cars to follow and overtake should aim to reduce this deficit.

REFERENCES

1. FIA, "2017 FIA Formula One Technical Regulations"2017.
2. Toet, W, "Aerodynamics and aerodynamic research in Formula 1" *Aeronautical Journal* 117(1187):1-26, 2013.
3. Agathangelou, B; Gascoyne, M, "Aerodynamic Design Considerations of a Formula 1 Racing Car" SAE Paper 980399, 1998.
4. Nakagawa, M., Kallweit, S., Michaux, F., and Hojo, T., "Typical Velocity Fields and Vortical Structures around a Formula One Car, based on Experimental Investigations using Particle Image Velocimetry," *SAE Int. J. Passeng. Cars - Mech. Syst.* 9(2):754-771, 2016, doi:10.4271/2016-01-1611.
5. Larsson, T; Sato, T; Ullbrand, B, "Supercomputing in F1 - Unlocking the Power of CFD"EACC, 6-7 July 2009 2005.
6. Larsson, T, "2009 Formula One Aerodynamics" 4th European Automotive Simulation Conference, Munich, Germany, 6-7 July 2009, 2009.
7. Ogawa, A; Yano, S; Mashio, S; Takiguchi, T; Nakamura, S; Shingai, M, "Development Methodologies for Formula One Aerodynamics" Development Methodologies for Formula One Aerodynamics, Honda R&D Technical Review 2009, F1 Special (The Third Era Activities) 2009.
8. Ogawa, A; Mashio, S; Nakamura, S; Masumitsu, Y; Minagawa, M; Nakai, Y, "Aerodynamics Analysis of Formula One Vehicles" Development Methodologies for Formula One Aerodynamics, Honda R&D Technical Review 2009, F1 Special (The Third Era Activities) 2009.

9. Dominy, J; Dominy, RG, "Aerodynamic influences on the performance of the Grand Prix racing car" *Proceedings of the Institution of Mechanical Engineers, Part D: Journal of Automobile Engineering* 198(2):87-93, 1984.
10. Zhang, X; Toet, W; Zerihan, J, "Ground effect aerodynamics of race cars" *Applied Mechanics Reviews* 59(1):33-49, 2006.
11. Katz, J, "Aerodynamics of race cars" *Annu. Rev. Fluid Mech.* 38:27-63, 2006.
12. Wilson, M., Dominy, R., and Straker, A., "The Aerodynamic Characteristics of a Race Car Wing Operating in a Wake," *SAE Int. J. Passeng. Cars - Mech. Syst.* 1(1):552-559, 2009, doi:10.4271/2008-01-0658.
13. Watts, M. and Watkins, S., "Aerodynamic Structure and Development of Formula 1 Racing Car Wakes," *SAE Int. J. Passeng. Cars - Mech. Syst.* 7(3):1096-1105, 2014, doi:10.4271/2014-01-0600.
14. Dominy, RG, "The influence of slipstreaming on the performance of a Grand Prix racing car" *Proceedings of the Institution of Mechanical Engineers, Part D: Journal of Automobile Engineering* 204(1):35-40, 1990.
15. Perry, R; Marshall, D, "An Evaluation of Proposed Formula 1 Aerodynamic Regulations Changes Using Computational Fluid Dynamics" 26th AIAA Applied Aerodynamics Conference, 2008.
16. Howell, J, "Catastrophic lift forces on racing cars" *Journal of Wind Engineering and Industrial Aerodynamics* 9(1-2):145-154, 1981.
17. Dominy, RG; Ryan, A; Sims-Williams, DB, "The influence of slipstreaming on sports prototype race car performance" *Proceedings of the Institution of Mechanical Engineers, Part D: Journal of Automobile Engineering* 214(8):887-894, 2000.
18. Dominy, R., LeGood, G., and Aerodynamics, G., "The use of a Bluff Body Wake Generator for Wind Tunnel Studies of NASCAR Drafting Aerodynamics," *SAE Int. J. Passeng. Cars - Mech. Syst.* 1(1):1404-1410, 2009, doi:10.4271/2008-01-2990.
19. McClintock, W, "The Aerodynamic Influence of Slipstreaming on a Formula One Race Car" Masters Thesis, Durham Univeristy, 2013
20. Soso, M, "Wings In Ground Effect" PhD Thesis, Univeristy of Illinois, 2002
21. Soso, M; Wilson, P, "Aerodynamics of a wing in ground effect in generic racing car wake flows" *Proceedings of the Institution of Mechanical Engineers, Part D: Journal of Automobile Engineering* 220(1):1-13, 2006.
22. Straker, A, "The influence of slipstreaming on racing car wing performance" Masters Thesis, Durham Univeristy, 2007
23. Soso, M; Wilson, P, "The influence of an upstream diffuser on a downstream wing in ground effect" *Proceedings of the Institution of Mechanical Engineers, Part D: Journal of Automobile Engineering* 222(4):551-563, 2008.
24. Correia, J; Roberts, L; Finnis, M; Knowles, K, "Aerodynamic characteristics of a monoposto racing car front wing operating in high turbulence conditions" The International Vehicle Aerodynamics Conference, Loughborough, 2014.
25. Newbon, JJ; Sims-Williams, DB; Dominy, RG, "Investigation into the Effect of the Wake from a Generic Formula 1 Car on a Downstream Vehicle" ISBN: 9780081001998, International Vehicle Aerodynamics Conference, Loughborough, 2014.
26. FIA, "2011 FIA Formula One Technical Regulations"2011.
27. SAE International Surface Vehicle Recommended Practice, "Vehicle Aerodynamics Terminology," SAE Standard J1594, Rev. July 2010.
28. Newbon, J., Dominy, R., and Sims-Williams, D., "CFD Investigation of the Effect of the Salient Flow Features in the Wake of a Generic Open-Wheel Race Car," *SAE Int. J. Passeng. Cars - Mech. Syst.* 8(1):217-232, 2015, doi:10.4271/2015-01-1539.

ACKNOWLEDGMENTS

The authors are grateful to Jaguar Land Rover and the EXA Corporation for the use of the PowerFLOW software suite. This research was supported by the Engineering and Physical Sciences Research Council (EPSRC).

DEFINITIONS/ABBREVIATIONS

α - wing incidence

θ - car pitch/rake angle

λ - wing aspect ratio

ρ - density of air at sea level

b - wing span

c - wing chord

$\mathbf{C_D}$ - aerodynamic drag coefficient

$\mathbf{-C_L}$ - aerodynamic downforce coefficient

$\mathbf{-C_{Lf}}$ - aerodynamic downforce, acting on front axle

$\mathbf{C_P}$ - static pressure coefficient

$\mathbf{h_{min}}$ - nominal ground clearance

H - car height dimension

L - car length dimension

P - static pressure

q - dynamic pressure

t - time

TI - turbulence intensity

u - velocity

W - car width dimension

SUBSCRIPTS:

x, y, z - Cartesian coordinate system

∞ - freestream

APPENDIX

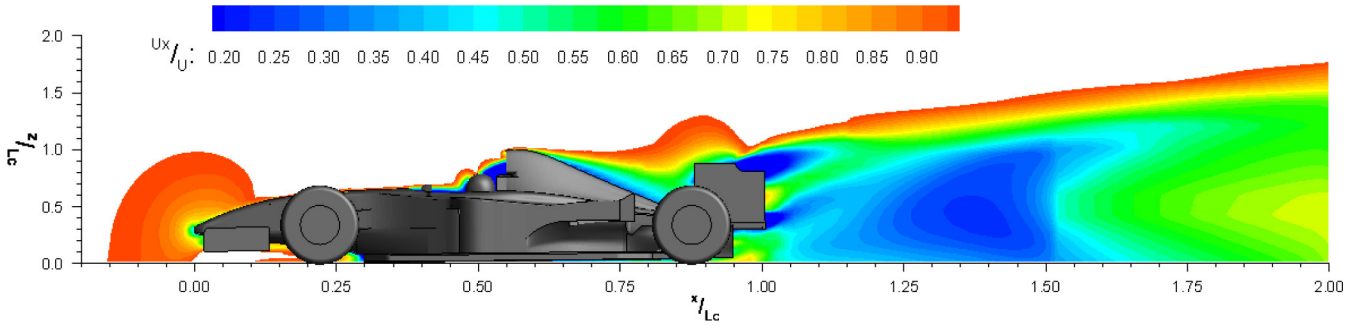

Figure 15. Centerline (y = 0) contours of axial velocity in wake

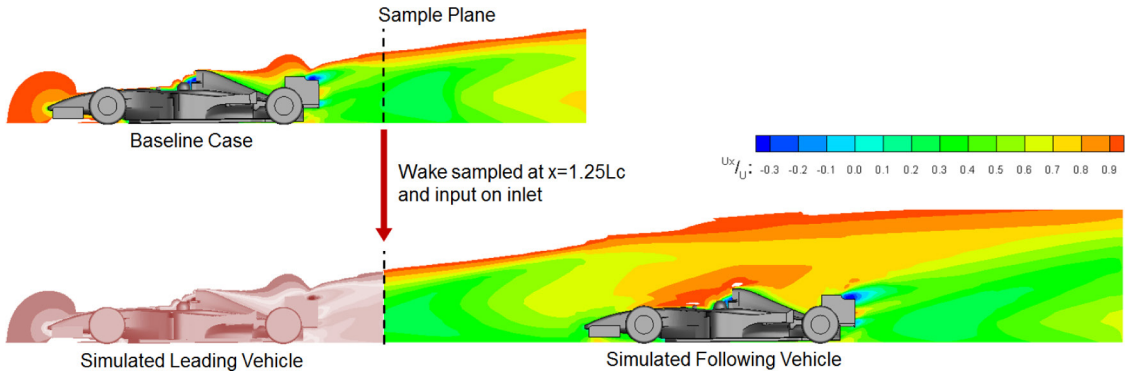

Figure 16. Method of imposing sampled wake on inlet plane of CFD case

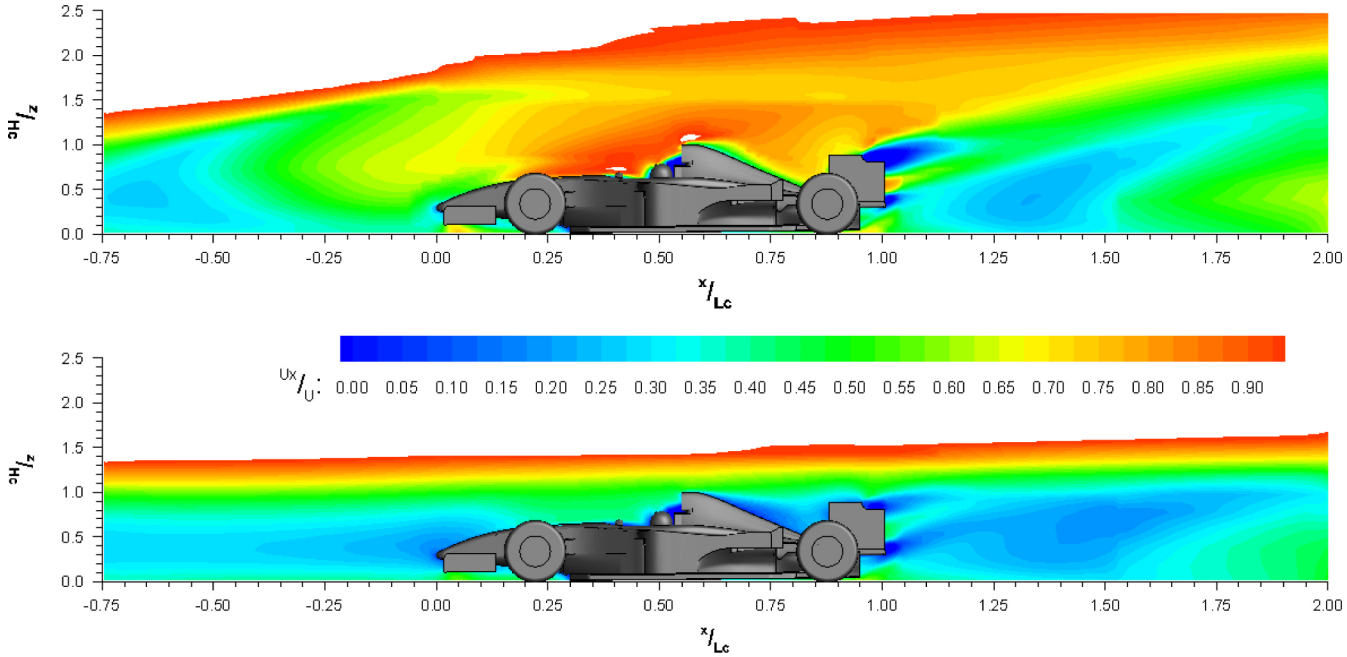

Figure 17. Centerline velocity contours, imposed wake case (upper) and secondary flows removed from upstream vehicle wake (lower)